Petrology and structure of syenite intrusions of the Okenyenya igneous complex

R.T. Watkins and A.P. le Roex

Department of Geology, University of Cape Town, Rondebosch 7700, South Africa

Intermediate and acid igneous rocks of the late-Mesozoic Okenyenya (Okonjeje) igneous complex, Namibia, are almost exclusively syenitic in composition. Microgranite occurs only as rare dykes and sills. Two rock types, syenite and quartz syenite, are readily distinguishable on petrographical and chemical grounds. They form very numerous intrusions including a circular peripheral ring dyke 4.5 km in diameter and are interpreted as being subvolcanic in origin. A close structural relationship is inferred between the ring dyke and an intricate series of subparallel curved intrusive sheets in the southwestern part of the complex. It is suggested that the latter formed through the injection of syenitic magmas into fractures developed in a foundering central block as a result of cauldron subsidence along the ring fault. Significant variations in composition between the two intrusive rock types, and the markedly heterogeneous character of the quartz syenite, may be explained by the tapping of a differentiated and contaminated magma chamber.

Introduction

The Okenyenya igneous complex (SACS, 1980),90 km northwest of Omaruru, is one of a series of late-Mesozoic igneous centres in Damaraland, Namibia (Fig. 1). It has previously been described under the name of Okonjeje (Korn & Martin, 1939, Simpson 1950, 1952 and 1954). The roughly circular complex, approximately 20 km² in area, contains a great diversity of igneous rocks ranging in composition from silica-undersaturated and strongly alkaline types through tholeiitic gabbros to quartz syenites and rare microgranites. This paper addresses the composition and structure of intrusions of silica saturated and oversaturated syenites. Younger silica-undersaturated (nepheline-) syenites which build the major peak of Okenyenya Berg (1902 m) (Fig. 2), and contact melted Damaran metasediments occurring locally at the margin of the intrusive complex, are not discussed.

In the only previous, detailed geological accounts of Okenyenya, Simpson (1950, 1952, 1954) variously termed the most silica-rich igneous rocks of the complex "ridge syenite", "marginal acid" and "hybrid rocks". On the geological map compiled by Simpson (1952,1954), "marginal acid and hybrid rocks" are depicted as a narrow outcrop around the eastern and southern margins as well as extensive continuous exposures in the western half of the complex. Simpson suggested these rocks, which in large part are strikingly heterogeneous in appearance, were emplaced as a thin carapace around older gabbroic intrusions. The petrology of these rocks and the mechanisms by which the "hybridisation" occurred were little discussed, although Simpson (1952, 1954) identified the most abundant xenoliths in the contaminated syenite as angular fragments of ferrogabbro and noted the partial assimilation of these host rocks by the acid magma.

The present study, part of our current reinvestigation of the Okenyenya igneous complex, aims to provide a more complete examination of the "acid" intrusions,
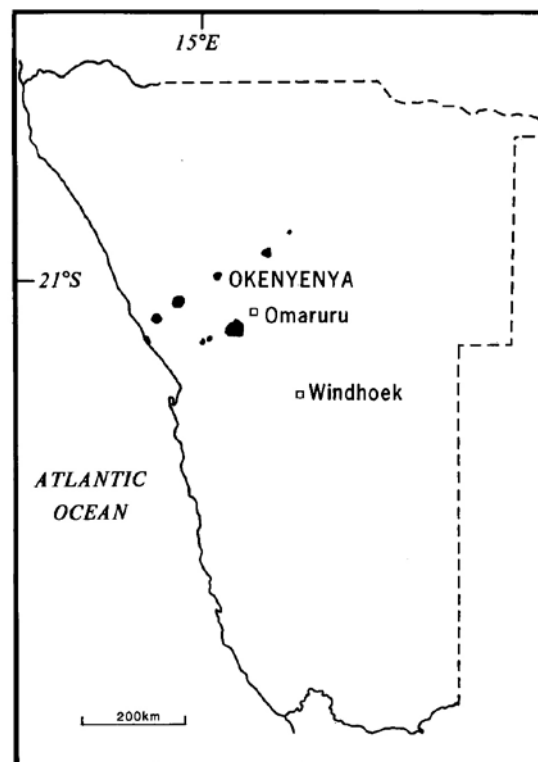

Fig. 1: Location of Okenyenya igneous complex in Damaraland, northeastern Namibia. Late-Mesozoic igneous complexes in Damaraland are shaded black.

which are significant in volume and of importance in the magmatic and structural evolution of the complex. It provides a simplified classification of the various intermediate and acid rocks and an alternative model of emplacement related to a cauldron subsidence of a former Okenyenya volcano.

Intrusive relations

Considerable solid rock outcrop and generally sparse vegetation over the complex have facilitated the map-
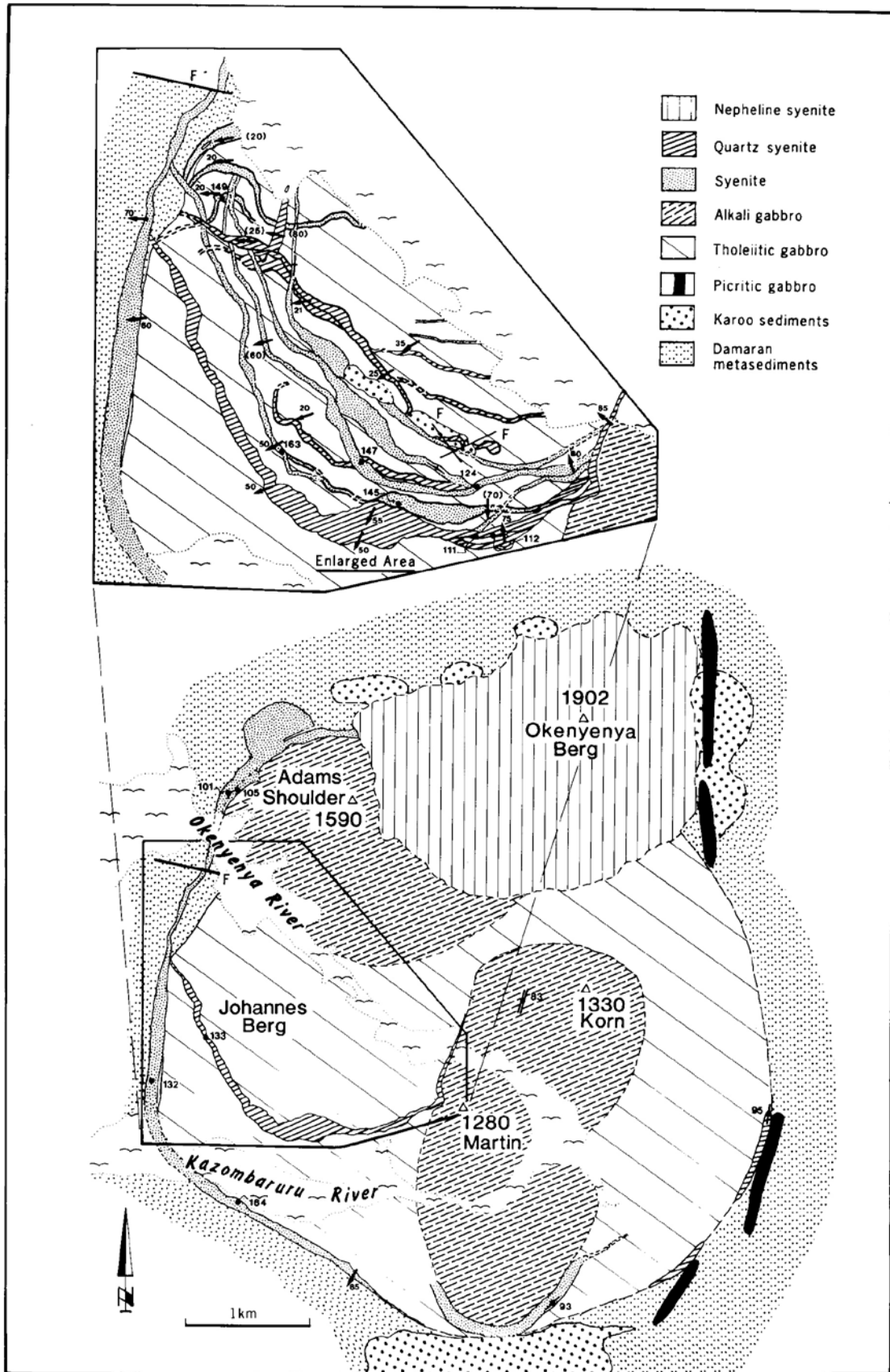
Fig. 2: The main syenitic intrusions of Okenyenya igneous complex. The extent of alkali gabbro and nepheline syenite intrusions are approximate. Detailed outcrop of the intrusions of Johannes Berg are shown in the INSET with only the "outer" arcuate dyke depicted on the main figure. Arrows indicate dip of the intrusive sheet in degrees; solid circles indicate locations of samples reported on in Tables 1 to 8.
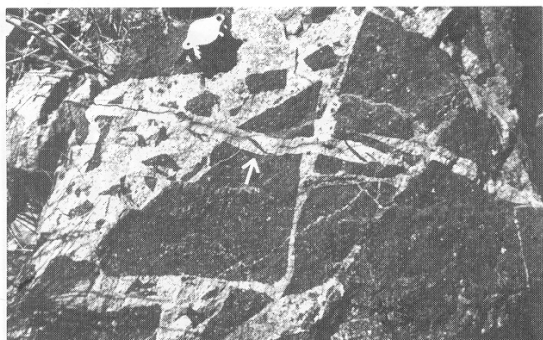
Fig. 3: Characteristic boundary of a syenite dyke on Johannes Berg. The margin of the dyke, on the left of the picture, contains numerous angular xenoliths of coarse-grained tholeiitic gabbro. The gabbro wall rocks are brecciated adjacent to the dyke and are penetrated by fine syenite veinlets. In this case, a late syenite vein (arrowed) cuts both the wall rocks and the syenite dyke and was probably intruded at a late stage in the solidification of the dyke. Hand lens for scale.

ping of numerous discrete syenite intrusions (Fig. 2). Difficulties were experienced in recognizing precise boundaries of the intrusions in some localities where there has been significant metasomatism of gabbroic country rock. The metasomatism which locally accompanies syenite intrusion, but appears more generally to relate to a later period of alkaline (lamprophyric) magmatism, has largely obscured former gabbroic textures. Distinguishing in the field between syenite and metasomatically altered gabbro is particularly difficult where the latter is a feldspar cumulate or is otherwise highly evolved and rich in feldspar, and it is apparent that significant exposures of metasomatised gabbro were misinterpreted as acid rocks on the original geological map (Simpson 1952, 1954).

A feature common to all the major syenite intrusions is the presence in the marginal zones of abundant xenoliths, along with brecciation of adjacent host rocks and their invasion by narrow syenite dykelers (Fig. 3). The syenite is frequently finer grained towards the margins of the intrusions and in the narrow apophyses, but very fine-grained or glassy chilled margins are not observed. A majority of the xenoliths in the marginal zones match the gabbro wall rocks, and fragments of Damaran metasedimentary rocks and Karoo lithologies are relatively rare. The gabbro xenoliths are mostly subangular, with narrow reaction coronas around some providing evidence of a degree of magmatic corrosion.

A second consistent feature of the syenite intrusions is their curvilinear outcrop. They may be grouped conveniently into three structural entities: a peripheral ring dyke, the "ridge syenite", and a complex series of sheet intrusions on the hill of Johannes Berg (Fig. 2).

Peripheral ring dyke

A roughly circular ring dyke, some 4.5 km in diameter, approximately delimits the igneous complex at the present level of exposure. The dyke is well developed around the WSW margin of the complex, where it attains a maximum thickness of some 75 m (Fig. 2) and comprises dominantly syenite of similar appearance to the "ridge syenite" described by Simpson (1952, 1954). Locally other intrusive sheets have been emplaced alongside the main dyke. The ring dyke extends to the ridge of Zebra Kop on the northern side of the Okenyenya River, where it is only slightly less broad and where it is accompanied by a plug-like body of syenite, approximately 280 x 500 m in outcrop (Fig. 2). The plug's contact with Damaran rocks dips at -80° towards the intrusion and has a 5 m wide margin of finer grained syenite. A narrow screen of highly altered gabbro partially separates the plug from the continuation of the ring dyke. To the north, the ring dyke narrows in exposures on the steep western flank of Okenyenya Berg before being truncated by the younger nepheline syenite intrusion.

The dyke also narrows south of the Kazombaruru River, but nevertheless can be traced along sporadic outcrops onto the steep northern slopes of Otjivero where it verges on the "ridge syenite" at the southern most edge of the igneous complex (Fig. 2). East of this point, impersistent exposures of syenite or merely gabbro showing much syenite veining mark the continuation of the feature around the eastern periphery of the complex. Additional evidence of the presence of a ring fracture may lie in the abrupt northwards termination of dykes of picritic gabbro on the southeastern rim of the complex (Fig. 2).

The relatively steep dip of the ring dyke is apparent from its surface trace. Precise measurement is invariably difficult, but the dyke appears to be close to vertical or to dip steeply inwards around much of the complex. On the western side of the complex, however, it appears from exposed margins and major joint sets to have a rather shallower outward dip of 60 - 70°.

The "ridge syenite"

As far as can be ascertained from field evidence, the "ridge syenite" is a separate intrusion from the major ring dyke. It demonstrably has a near-vertical dip and narrows abruptly at its north-facing ends, as previously described (Simpson, 1952, 1954). A zone of syenitic veining within the gabbros adjacent to the wall-like termination of the eastern limb (Fig. 2) indicates a possible continuation of the fracture occupied by the syenite dyke. Erosion of a broad stream valley on the northern side of the Kazombururu River valley (Fig. 2) might mark an extension of the fracture to the northwest, although this must remain speculative in the absence of satisfactory exposure amongst the talus and alluvium.

Johannes Berg syenite sheets

Numerous intrusive syenite sheets have been identi-

fied cutting the gabbros of Johannes Berg (Fig. 2) and it is here that the present structural interpretation differs profoundly from the earlier interpretation (Simpson, 1954). A series of low ridges extending obliquely across the crest of the elongate Johannes Berg mountain are formed by closely spaced syenite dykes (Fig. 2) or, less frequently, by resistant gabbro screens between the syenite intrusions. The dykes, which number at least six, have subparallel arcuate outcrop (Fig. 2).

A major dyke, which for the most part is the outermost of the series, is a distinctive pink, quartz-rich rock that practically throughout contains subangular to rounded blebs of a darker, more mafic material (Fig. 4a, 4b). These enclaves generally vary from microscopic to a few centimetres in size. However, locally in the dyke, rounded lobes of fine-grained, bluish-grey rock, many metres across, interfinger with the pink syenite (Fig. 4c). The extraneous rock, composed dominantly of biotite, alkali feldspar and Fe-Ti oxide, has a distinctive felted texture and is not seen elsewhere in the igneous complex. Interpenetrating relations, including possible

diapiric intrusion of the syenite into the more mafic bodies, crenulated boundaries (Fig. 4b), and unusually extensive zones of reaction around the mafic bodies, are suggestive of the coexistence of two different magmas. The dyke has an outward dip of close to 55° along much of its length, although it steepens towards its ends, appearing vertical or even overturned at its eastern extremity. A thickness of -15 m along its central section lessens to around 10 m towards both ends.

Other dykes of the series, though generally somewhat narrower (5 - 10 m), share the same 50 - 55° outward dip in their central sections and parallel the outermost dyke. Occasionally a dyke may be seen to terminate against or extend alongside a neighbouring dyke; less frequently, two dykes appear to cross. At the western end of Johannes Berg, the outer dykes of the series extend to the ring fracture (Fig. 2), while the remainder are obscured by surface lag deposits and alluvium of the Okenyenya River. In the east, the dykes converge in exposures on the sides of a valley separating Johannes Berg and the peak of Martin (Fig. 2). Here the relation-
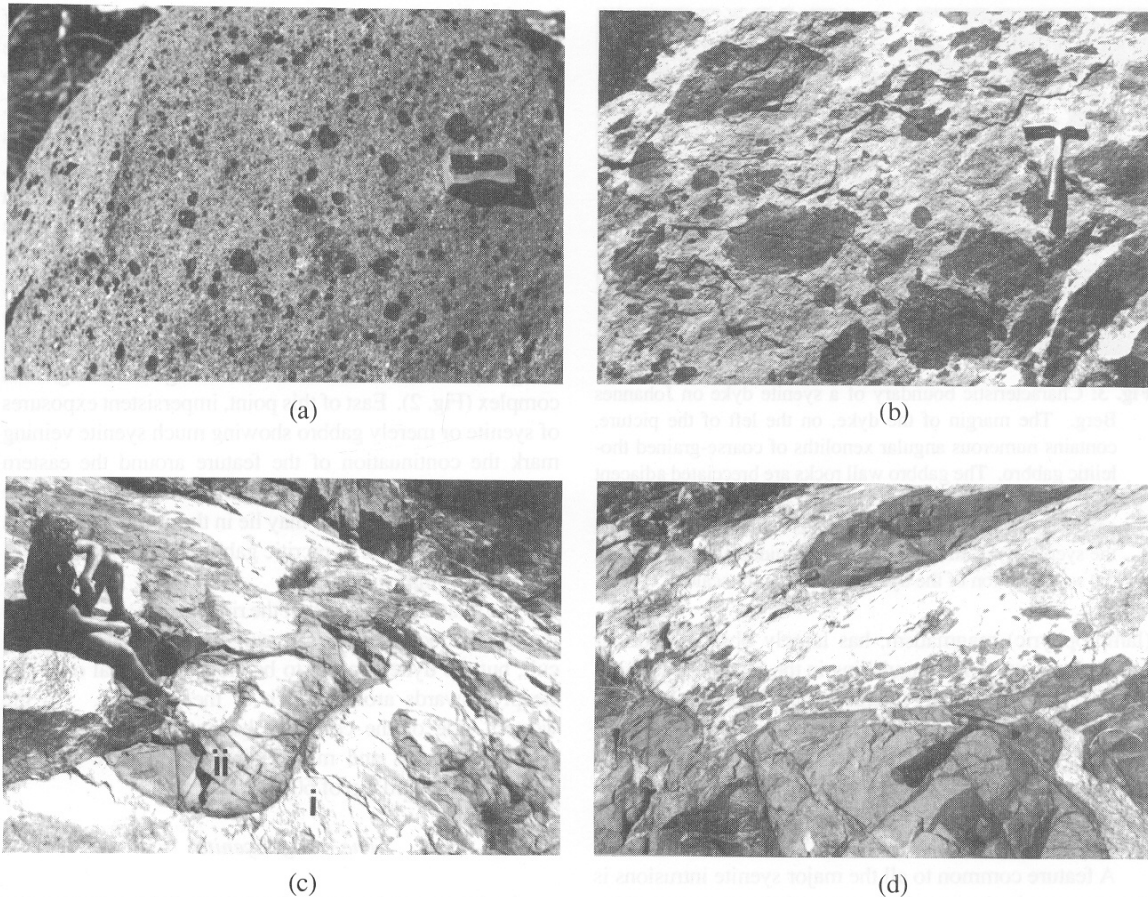

(a)

(b)

(c)

(d)

Fig. 4: Heterogeneous character of the *quartz syenite* intrusions. (a) Typical "contaminated" appearance of the *quartz syenite* with extremely abundant xenocrysts of dark amphibole and aggregates of biotite. Pencil sharpener for scale. (b) Abundant bodies of mafic rock in lighter coloured *quartz syenite*. Note the highly irregular and crenulated boundaries. Hammer for scale. (c) Large-scale interpenetrative relations between lighter coloured (pink) *quartz syenite* (i) and darker (pale blue-grey) more mafic rock (ii) in the "outer" arcuate dyke, Johannes Berg. Note the dark, fine-grained, rounded margin of the mafic body, a result of chilling or reaction. (d) Disintegration of mafic body in contact with pale *quartz syenite*. The mafic rock shows signs of both brittle hydraulic fracture and more plastic deformation. Hammer for scale.

ship between individual intrusive sheets is not easily determinable, but inner members of the series appear to terminate against the outer (pink syenite) dyke. This dyke then extends northwards into the Okenyenya River valley as a single sheet which narrows and eventually gives way to a zone in which the leucocratic syenite is reduced to narrow veins within intensely metasomatised gabbro. Whilst showing a close structural relationship, individual dykes of Johannes Berg are composed of syenite of contrast-ing compositions (Fig. 2) - see later discussion.

A second group of intrusive syenite sheets, again including contrasting syenite compositions, cut the gabbros of Johannes Berg at a more shallow angle, generally <30° (Fig. 2). Their dip is more erratic than that of the dykes, steepening in places to 40° or 50°, but is almost entirely outward from the centre of the complex. These sheets are mostly thinner, <5 m, than the dykes

TABLE 1: Major oxides, CIPW norms, and modal compositions of representative acid rocks from Okenyenya igneous complex. Sample localities are shown in Fig. 2. *$Fe_2O_3/FeO = 0.2$. Modal compositions are estimated from the counting of 1500 points on single thin sections; [1]discrete crystals of multiply twinned oligoclase and sodic-andesine; [2]resolvable crystals of sericite and epidote; [3]altered fayalite = iddingsite and chlorite; [4]iron-titanium oxides and secondary pyrite; [5]discrete chlorite, replacing amphibole and biotite. The greater degree of alteration of feldspar from the *quartz syenites* to sericite is not reflected in the modal analyses owing to the extremely fine grain size of the secondary mineral.

	SYENITES					QUARTZ SYENITES				MICRO-GRANITE
Sample No.	OKJ 93	OKJ 105	OKJ 132	OKJ 163	OKJ 149	OKJ 112	OKJ 133	OKJ 101	OKJ 95	OKJ 83
SiO_2	59.69	58.42	62.24	62.12	62.51	64.56	66.09	68.29	68.68	72.18
TiO_2	0.87	1.16	0.90	0.80	0.86	0.37	0.43	0.60	0.45	0.25
Al_2O_3	16.55	16.15	15.52	16.31	16.11	18.15	15.29	14.67	14.57	14.48
Fe_2O_3*	1.27	1.09	0.91	0.74	0.95	0.46	0.49	0.61	0.71	0.25
FeO	6.38	5.44	6.10	4.95	4.74	2.31	3.25	3.03	3.54	1.24
MnO	0.24	0.18	0.23	0.23	0.23	0.07	0.10	0.09	0.11	0.02
MgO	0.62	1.87	0.67	0.55	0.72	0.44	0.45	0.86	0.30	0.19
CaO	2.93	4.22	2.65	1.72	1.88	1.18	1.42	2.41	1.53	0.22
Na_2O	5.11	4.36	4.42	5.53	5.12	5.52	4.82	3.57	3.79	3.82
K_2O	5.77	4.08	5.26	6.16	5.99	6.79	5.78	5.08	5.89	7.33
P_2O_5	0.20	0.34	0.20	0.16	0.17	0.14	0.08	0.17	0.06	0.04
L.O.I.	1.08	2.42	0.62	0.96	1.01	0.39	1.30	0.65	0.84	0.71
TOTAL	100.70	99.73	99.72	100.23	100.29	100.40	99.50	100.03	100.47	100.73
CIPW NORMS										
Qz	-	4.26	7.02	0.16	2.84	2.84	10.83	20.36	18.28	20.41
Or	34.04	24.05	31.02	36.40	35.34	40.12	33.98	30.02	34.81	43.26
Ab	43.15	36.81	37.32	46.79	43.24	46.71	40.53	30.21	32.07	32.32
An	5.17	12.44	6.94	1.46	3.26	4.67	2.99	8.95	5.32	0.69
Di	6.99	5.25	4.22	5.24	4.27	0.24	3.01	1.61	1.64	0.12
Hy	0.91	10.10	8.83	6.22	7.02	4.60	4.56	5.90	5.65	2.25
Ol	5.59	-	-	-	-	-	-	-	-	-
Mt	1.44	1.23	1.32	1.08	1.07	0.52	0.71	0.69	0.80	0.28
Il	1.65	2.20	1.71	1.52	1.63	0.70	0.82	1.14	0.85	0.47
Ap	0.47	0.81	0.47	0.38	0.40	0.33	0.19	0.40	0.14	0.09
MODAL COMPOSITION										
Qtz	0.2	1.5	7.5	-	1.9	0.4	5.0	11.1	17.5	18.8
Alk Fsp	78.9	68.8	76.7	79.8	83.4	88.6	82.8	68.0	63.1	76.0
Plag[1]	6.1	8.9	3.8	1.3	2.8	3.7	2.9	9.4	7.1	2.4
Ser/Epid[2]	2.2	7.5	1.8	2.1	2.1	0.3	0.5	0.2	1.9	0.9
Fayalite	0.4	0.3	1.3	0.7	1.6	-	-	0.1	-	-
alt Fay[3]	0.3	0.1	0.3	0.1	1.5	-	-	-	-	-
Cpx	7.5	2.6	2.0	7.9	1.0	tr	0.1	-	0.3	0.2
Opx	0.1	-	0.1	tr	-	tr	-	0.3	-	-
Amph	0.6	2.5	3.0	3.0	2.6	5.5	7.0	-	5.9	-
Biotite	0.2	1.0	0.2	0.2	-	0.1	-	5.3	0.8	-
FeTi[4]	2.5	2.9	2.0	3.8	1.9	0.8	1.3	3.9	2.4	1.0
Apatite	0.3	0.9	0.3	0.7	0.5	0.3	0.1	1.2	0.2	tr
Chl[5]	0.4	2.7	0.4	-	0.4	0.1	-	0.4	0.2	0.2
Calcite	0.2	0.3	-	0.1	0.2	tr	-	-	-	-

and more variable in their thickness of outcrop. Like the dykes, they form a subparallel series of intrusions with individual sheets in places juxtaposed. At the western end of Johannes Berg, members of this series are seen to intersect the more steeply dipping dykes, with either dykes or shallow-dipping sheets cross-cutting, and, in one case, a dyke is apparently continuous with a shallow-dipping sheet.

Petrology

Analytical methods

Modal analyses of syenite rocks were estimated by point counting on single microscope thin sections. Quantitative mineral analyses were performed on the Cameca/Camebax Microbeam electron microprobe in the Department of Geochemistry, University of Cape Town, using natural mineral standards. On-line data reduction was carried out using the correction programme of Bence & Albee (1968) with alpha factors of Albee & Ray (1970). Whole-rock major element analyses were performed by X-ray fluorescence using the standard technique of Norrish & Hutton (1969). Trace elements, and sodium, were analysed using sample powder briquettes. Sample sizes were approximately 2 kg, and analytical procedures and conditions were essentially similar to those described by Duncan *et al.* (1984). Rare-earth elements were determined by gradient ion chromatography using a DIONEX 4000i ion chromatograph (le Roex & Watkins, 1990).

Rock classification

Major element compositions, calculated normative compositions, and estimated modal analyses of samples representative of the full range of intermediate and acid intrusive rock types from Okenyenya are given in Table 1. All of these rocks consist dominantly of microperthitic orthoclase showing various degrees of exsolution. Plagioclase, generally oligoclase, occurs in subordinate amounts as discrete crystals. All rocks are highly leucocratic with ferromagnesian minerals and iron-titanium oxides accounting for ≤ 10 modal %. Quartz is present in most samples, but varies significantly in amount from sparse crystals <1 %) to as much as 19 modal % (Table 1).

Based upon the modal estimates, all of the rocks in the present study may be classified as syenites or quartz syenites according to the IUGS scheme for plutonic rocks (Streckeisen, 1973; Le Maitre, 1989). If the calculated normative compositions are employed, a small number of samples (e.g. OKJ-95, OKJ-101; Table 1) fall just within the field of granite. There is, nevertheless, a clear continuum between these samples and the remainder in the study, a fact underlined by the localised occurrence of quartz-rich "granitic" pegmatites within some quartz syenite sheets. Otherwise, only in the case of minor dykes recording the very highest SiO_2 contents of intrusive rocks from the complex, is the normative quartz sufficient to place the rock significantly in the granite field. These rocks, an example of which is a narrow dyke OKJ-83 (Table 1) in which quartz forms 23% of normalised Q-A-P components, show significant

TABLE 2: Representative feldspar analyses from *syenite* and *quartz syenite* of the Okenyenya igneous complex. FeO* = total iron as FeO; nd = not detected.

	Feldspar Analyses									
	Syenite					Quartz Syenite				
	1	2	3	4	5	6	7	8	9	10
SiO_2	66.03	67.58	65.14	64.92	67.14	60.58	64.82	67.49	67.01	65.31
Al_2O_3	20.66	20.59	18.04	19.40	19.31	25.30	21.72	18.36	18.78	18.31
FeO*	nd	nd	0.56	nd	0.20	nd	nd	nd	nd	0.20
MgO	nd	nd	nd	nd	-	nd	nd	nd	nd	nd
CaO	2.27	1.58	0.01	1.33	1.06	7.92	3.53	0.42	0.33	0.14
Na_2O	9.94	9.90	1.89	5.79	7.80	6.75	9.45	7.64	4.99	1.88
K_2O	0.25	0.39	13.48	7.44	4.10	0.24	0.32	5.08	8.98	13.59
Total	99.15	100.04	99.11	98.90	99.61	100.79	99.82	98.99	100.09	99.43
An	11.0	7.9	0.01	6.4	5.3	38.8	16.8	2.0	1.7	0.7
Ab	87.5	89.8	17.6	50.7	70.4	59.8	81.4	68.1	45.0	17.2
Or	1.5	2.3	82.4	42.9	24.3	1.4	1.8	29.9	53.3	82.1

1. Plagioclase - core (OKJ-93)
2. Plagioclase - core (OKJ-122)
3. Alkali feldspar (OKJ-122)
4. Alkali feldspar - core (OKJ-132)
5. Alkali feldspar - core (OKJ-122)

6. Plagioclase - small euhdral (OKJ-115)
7. Plagioclase - core (OKJ-111)
8. Alkali feldspar - phenocryst (OKJ-168)
9. Alkali feldspar - phenocryst core (OKJ-112)
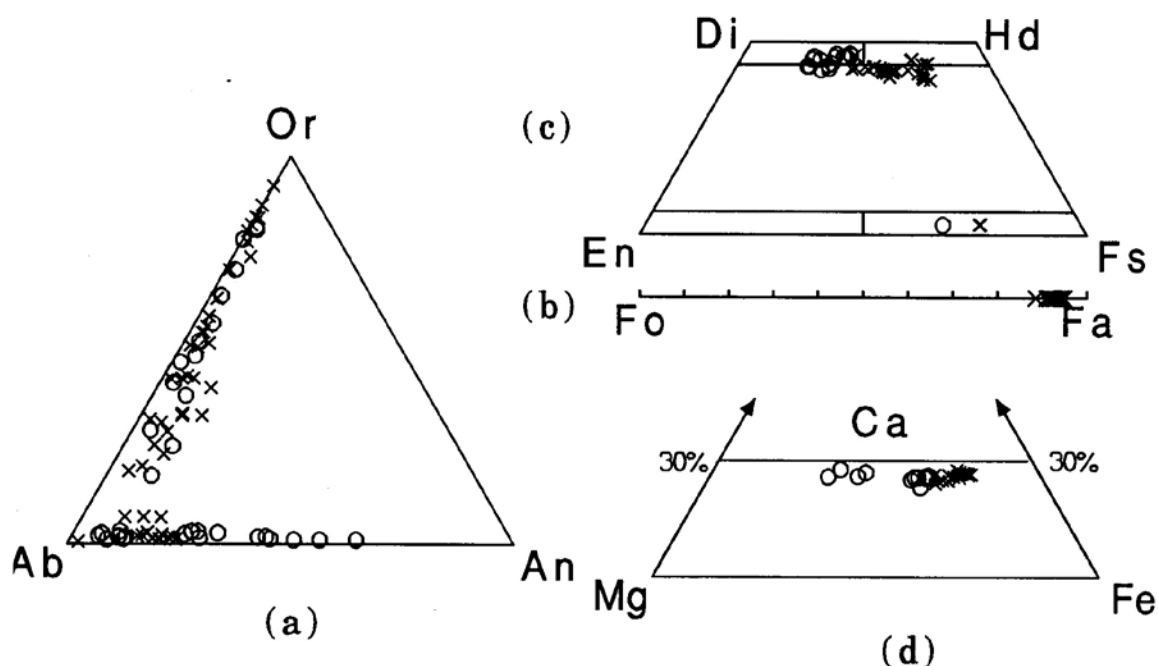10. Alkali feldspar - phenocryst (OKJ-166)

Fig. 5: Mineral compositions from syenitic rocks: (a) feldspars; (b) olivines; (c) pyroxenes; (d) amphiboles. Minerals from *syenites* are shown as crosses and those from *quartz syenites* as open circles. Labradoritic plagioclase, diopsidic pyroxene and the most Ca-rich amphibole compositions in the *quartz syenites* are interpreted as being xenocrysts of gabbroic origin.

chemical and mineralogical differences from the other rocks of the study and may appropriately be termed microgranites. Other quartz-rich rocks have been produced locally at the contact of the intrusive complex by the recrystallisation or partial melting of sandstones and metasedimentary rocks.

The intrusive syenites from Okenyenya may be divided into two distinct types on the basis of petrography and mineralogy, as well as aspects of their major and trace element compositions. This division corresponds very closely, although not precisely, to that between syenite and quartz syenite, as defined by the IUGS classification (le Maitre 1989). To facilitate discussion in the remainder of this paper, the two dominant rock types will hereafter be termed *syenite* and *quartz syenite*, despite the presence of rare examples in each group which are incorrectly named in terms of a rigorous classification.

The "ridge syenite" (Simpson, 1954) is a typical example of the *syenite*, whilst the distinctive pink rock of the outer arcuate dyke on Johannes Berg (Fig. 2) exemplifies the *quartz syenite*. Specific differences between the two rock types are discussed within the following sections.

Petrography and mineral chemistry

Some 400 mineral analyses are available from samples of the syenite intrusions. Representative analyses of the major minerals are presented in Tables 2 to 7. Compositional variations in selected minerals are shown in Fig. 5. Individual analyses are available from

the authors on request.

Syenites

Syenite forms the major injection of the ring dyke around the western perimeter of the complex, the "ridge syenite", and numerous steep- and shallow-dipping sheet intrusions of Johannes Berg. It is consequently the more voluminous of the two syenitic rock types. When fresh it is characteristically greenish-blue, coloured by the overwhelmingly dominant alkali feldspar. Crystal lamination occurs frequently towards the margins of intrusions but is absent from central portions which normally exhibit a roughly equigranular texture with interlocking anhedral feldspar crystals up to 3 mm in size. Away from the margins, the syenite contains only infrequent xenoliths. Crystal boundaries are mostly extremely irregular and include simplectic intergrowths. Less commonly this rock type exhibits a weak trachytic texture with abundant, simply-twinned, subhedral, alkali feldspar laths up to 3.5 mm in length. These have the appearance of small phenocrysts which lie in a groundmass of smaller feldspar laths, subhedral clinopyroxene and Fe- Ti oxides. Boundaries of both the feldspar phenocrysts and smaller laths are highly irregular. Margins and interior areas of the larger phenocrysts contain abundant clinopyroxene inclusions, the distribution of which mimics that in the groundmass, clearly indicating late partial recrystallisation and overgrowth in these phenocrysts.

The orthoclase microperthite exhibits coarse, irregular ex solution lamellae. The sodic plagioclase is frequently Ab_{97}, and may contain up to 20% of the An molecule

TABLE 3: Representative pyroxene analyses of *syenite* and *quartz syenite* of the Okenyenya igneous complex. Abbreviations as in Table 2.

	Pyroxene Analyses									
	Syenite						Quartz Syenite			
	1	2	3	4	5	6	7	8	9	10
SiO_2	50.85	49.83	49.87	48.43	48.34	51.33	48.80	50.38	49.97	50.67
TiO_2	0.11	0.30	0.57	0.06	0.20	0.69	0.11	0.57	0.40	0.72
Al_2O_3	0.32	0.48	0.97	0.13	0.50	1.59	0.25	1.55	0.92	2.23
FeO*	13.02	20.82	17.52	40.70	24.96	9.50	38.16	12.06	14.66	11.25
MnO	1.06	1.15	1.14	2.92	1.00	0.69	1.51	0.84	0.66	0.60
MgO	11.01	7.36	8.80	7.34	5.51	14.12	10.36	12.49	9.81	13.11
CaO	22.34	19.99	20.59	1.21	18.73	21.18	1.19	20.44	22.15	20.31
Na_2O	0.29	0.38	0.47	0.01	0.25	0.55	nd	0.60	0.64	0.88
Total	99.00	100.31	99.93	100.80	99.49	99.65	100.38	98.93	99.21	99.77
Wo	46.8	43.0	44.3	2.8	40.9	45.5	2.6	43.3	46.9	42.9
En	32.0	22.0	26.3	23.7	16.7	39.0	31.8	36.8	28.9	38.5
Fs	21.2	35.0	29.4	73.6	42.4	15.5	65.6	19.9	24.2	18.6

1. Large clinopyroxene core (OKJ-160)
2. Small clinopyroxene core (OKJ-149)
3. Small clinopyroxene core (OKJ-145)
4. Large subhedral orthopyroxene (OKJ-132)
5. Subhedral clinopyroxene (OKJ-132)
6. Clinopyroxene mantled by amphibole (OKJ-166)
7. Small corroded orthopyroxene (OKJ-115)
8. Small anhedral clinopyroxene (OKJ-166)
9. Small rounded clinopyroxene (OKJ-167)
10. Large clinopyroxene mantled by amphibole (OKJ-166)

(Fig. 5a). Oligoclase, and rarely sodie-andesine, occur in subordinate amounts in some samples as discrete anhedral to subhedrallaths or irregularly intergrown with larger orthoclase microperthite crystals. Sericitisation of the feldspar has proceeded to differing degrees, although some rocks are unusually free of such alteration. Quartz is present in small and variable amounts (Table 1) mostly as aggregates of anhedral crystals filling interstices between feldspar grains.

Corroded crystals of fayalite (Fo_5 - Fo_{11}: Table 4; Fig. 5b) <2 mm in size and invariably altered to iddingsite along fractures and rims, are a distinctive component of the *syenite*, frequently occurring in aggregates with ilmenite, clinopyroxene, rare orthopyroxene, amphibole and apatite. Iron-rich augite (En_{14-28} Fs_{27-43} Wo_{41-46}: Table 3) is present as anhedral to subhedral crystals <2 mm in size. Pyroxene compositions are shown in Fig. 5c. Amphibole of ferroedinite composition (Leake 1978) with Fe/(Fe + Mg) = 0.68-0.79 (Table 5; Fig. 5d) occurs as discrete crystals or as reaction mantles on fayalite and pyroxene. Biotite is normally present only in very subordinate amounts and again results from reaction at grain boundaries. llmenite ($Il_{96}Hm_4$ - $Il_{90}Hm_{10}$) is the dominant opaque phase, occurring most commonly as partially rounded, but otherwise well-formed equant grains (Table 6). Magnetite (Usp_5Mt_{95} - $Usp_{40}Mt_{60}$) is present as less well-formed, equant and platy crystals. Apatite, containing 5 - 7 wt % F (Table 7), is an abundant accessory phase.

TABLE 4: Representative olivine analyses from *syenite* of the Okenyenya igneous complex. Abbreviations as in Table 2.

	Olivine Analyses				
	Syenite				
	OKJ-145	OKJ-93	OKJ-132	OKJ-132	OKJ-149
SiO_2	30.32	29.34	29.84	29.45	29.43
FeO*	61.02	63.75	65.19	65.72	62.90
MnO	3.72	3.50	2.95	2.84	3.59
MgO	4.39	3.29	2.49	1.94	3.47
CaO	0.09	0.11	0.01	0.07	0.08
Total	99.54	99.99	100.47	100.02	99.47
Fo	11.4	8.5	6.4	5.04	9.02

Quartz syenites

The *quartz syenite* is generally less coarse-grained and less equigranular than the *syenite*. It forms a number of the sheet intrusions on Johannes Berg and minor injections along the ring fracture (Fig. 2). In place of the consistent blue-green colouration, there is variation in colour, mostly cream or pink, but also darker, bluish-grey in some cases. Specimens commonly exhibit an "altered" appearance due to the highly turbid nature of the alkali feldspar. Growth of exceedingly fine-grained sericite and epidote (not represented in the modal analyses in Table 1) is particularly prevalent in the exterior regions of the feldspar crystals. The dominant texture is one in which larger (max. -6 mm) subhedral to anhedral

TABLE 5: Representative amphibole analyses from *syenite* and *quartz syenite* of the Okenyenya igneous complex. Abbreviations as in Table 2.

	Amphibole Analyses							
	Syenite				Quartz Syenite			
	1	2	3	4	5	6	7	8
SiO$_2$	41.73	42.22	41.57	44.00	42.88	43.23	44.34	48.02
TiO$_2$	1.65	2.30	1.85	1.47	1.92	1.47	1.72	1.20
Al$_2$O$_3$	8.47	8.02	7.93	5.85	7.28	6.56	7.05	5.37
FeO*	27.17	25.02	28.88	27.47	28.12	26.75	24.03	17.88
MnO	0.57	0.84	0.70	0.94	0.91	0.97	0.62	0.56
MgO	5.97	7.10	4.26	6.09	5.20	5.03	8.37	12.45
CaO	10.54	10.31	10.26	9.90	10.40	10.35	10.52	10.98
Na$_2$O	1.90	2.21	2.08	2.20	2.28	2.02	2.07	1.80
K$_2$O	1.15	1.07	1.02	0.68	0.95	1.00	0.78	0.50
Total	99.15	99.09	98.55	98.60	99.94	97.38	99.50	98.76

1. Anhedral amphibole (OKJ-170)
2. Mantle on clinopyroxene (OKJ-122)
3. Anhedral amphibole (OKJ-132)
4. Anhedral amphibole (OKJ-149)

5. Large subhedral crystal (OKJ-111)
6. Small subhedral crystal (OKJ-112)
7. Large subhedral crystal (OKJ-115)
8. Reaction rim on clinopyroxene (OKJ-166)

TABLE 6: Selected biotite and apatite analyses from *syenite* and *quartz syenite* of the Okenyenya igneous complex. Totals have not been corrected for replacement of O by F in the mineral structure. Abbreviations as in Table 2.

	Biotite and Apatite Analyses							
	Syenite				Quartz Syenite			
	1	2	3	4	5	6	7	8
SiO$_2$	36.52	35.34	-	-	36.71	36.62	-	-
TiO$_2$	3.63	4.84	-	-	2.52	3.08	-	-
Al$_2$O$_3$	12.67	13.06	-	-	11.43	12.23	-	-
FeO*	24.80	23.34	-	-	31.06	28.11	-	0.30
MnO	0.20	0.33	-	-	0.42	0.30	-	-
MgO	9.53	9.08	-	-	6.19	7.37	-	-
CaO	0.07	0.01	54.50	54.21	nd	0.01	54.10	54.30
Na$_2$O	0.24	0.15	-	-	0.15	0.29	-	-
K$_2$O	8.98	8.94	-	-	8.25	8.84	-	-
P$_2$O$_5$	-	-	40.69	40.27	-	-	40.47	40.14
F	4.96	2.79	6.08	5.22	-	0.97	4.56	4.09
Cl	-	-	-	0.34	-	-	0.70	nd
Total	101.60	97.88	101.27	100.04	99.92	97.82	99.83	98.83

1. Biotite (OKJ-145)
2. Biotite (OKJ-160)
3. Apatite (OKJ-93)
4. Apatite (OKJ-122)

5. Biotite (OKJ-111)
6. Biotite (OKJ-115)
7. Apatite (OKJ-166)
8. Apatite (OKJ-166)

orthoclase microperthite crystals and less abundant plagioclase and quartz crystals lie in a matrix of smaller, but often well-formed, alkali feldspar crystals with interstitial albite and quartz.

Orthoclase microperthite crystals are frequently simply twinned; multiply twinned oligoclase (An$_{32}$; Table 2) occurs as quite large subhedrallaths (up to 2 mm) and smaller crystals intergrown with the orthoclase. Crystals of more calcic composition, up to An$_{64}$, are interpreted a.5 xenocrysts from gabbroic sources. Quartz is generally more abundant than in the *syenites*, occurring similarly as anhedral aggregates filling interstices between feldspar grains, but also commonly as only slightly rounded equidimensional and more strongly embayed crystals up to 1 mm in size. Localised pegmatitic areas contain quartz and orthoclase feldspar crystals >10 mm in size. Fayalite is absent, except for a trace in one sample (Table 1), and clinopyroxene, if present, occurs
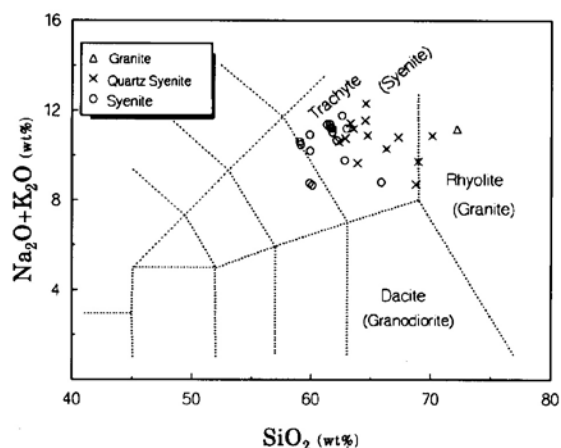
TABLE 7: Selected Fe-Ti oxide analyses from *syenite* and *quartz syenite* of the Okenyenya igneous complex. Fe_2O_{3c} and FeO_c have been calculated on the basis of stoichiometry. Other abbreviations as in Table 2.

	Oxide Analyses									
	Syenite					Quartz Syenite				
	1	2	3	4	5	6	7	8	9	10
SiO_2	nd	0.11	nd	0.09	nd	nd	nd	nd	nd	nd
TiO_2	50.77	11.91	47.45	1.54	51.22	50.44	1.03	50.42	48.10	3.76
Al_2O_3	nd	0.69	0.28	0.45	nd	-	nd	nd	nd	nd
FeO*	46.73	81.96	48.34	91.34	46.65	45.40	91.55	46.80	50.16	89.04
MnO	2.05	0.88	2.86	nd	2.06	3.86	nd	1.96	1.54	0.48
MgO	-	-	0.08	nd	-	0.06	nd	nd	0.06	-
Total	99.55	95.55	99.01	93.42	99.93	99.76	92.58	99.18	99.86	93.28
Fe_2O_{3c}	3.51	44.97	9.67	65.25	2.98	4.50	66.46	3.84	9.51	61.31
FeO_c	43.57	41.49	39.64	32.63	43.97	41.35	31.75	43.35	41.60	33.87
$Total_c$	99.93	100.07	99.99	99.98	100.26	100.23	99.28	99.59	100.83	99.45
	Il 97	Us 35	Il 90	Us 5	Il 97	Il 95	Us 3	Il 96	Il 91	Us 11
	Hm 3	Mt 65	Hm 10	Mt 95	Hm 3	Hm 5	Mt 97	Hm 4	Hm 9	Mt 89

1. Anhedral ilmenite (OKJ-93)
2. Anhedral titanomagnetite (OKJ-93)
3. Ilmenite lamellae in magnetite 4 (OKJ-122)
4. Magnetite host to ilmenite 3 (OKJ-122)
5. Anhedral ilmenite (OKJ-149)
6. Anhedral ilmenite (OKJ-167)
7. Anhedral magnetite (OKJ-167)
8. Anhedral magnetite (OKJ-115)
9. Ilmenite in reaction rim to clinopyroxene (OKJ-166)
10. Magnetite in reaction rim to clinopyroxene (OKJ-166)

only in trace amounts. Edenitic amphibole (Table 5; Fig. 5d) is the most abundant mafic phase, with significant biotite present in some samples. Ilmenite ($Il_{95}Hm_5$ - $Il_{98}Hm_2$) occurs as equant and bladed crystals but magnetite ($Usp_{11}Mt_{89}$ - Usp_1Mt_{99}), showing Ti-rich exsolution, forms the greater number of opaque crystals (Table 6). Secondary pyrite is common in some samples, at least in part replacing magnetite. Apatite is again conspicuous in many samples but appears neither to be present in such abundance, nor as crystals as large as in the syenite. A fluorine content of 3 - 4.5 wt % is lower than recorded from apatite in the syenite (Table 7).

A marked feature of the quartz syenites is the ubiquitous presence of dark inclusions (Fig. 4a). In addition to small xenoliths, mostly wall-rock gabbro, there are more abundant enclaves, many of a finer grained, paler coloured, mafic material which cannot be matched to other lithologies in the complex. The enclaves occur on all scales from lobate features, several metres in size, in the outer dyke on Johannes Berg (Fig. 4c), to small «1 mm) rounded aggregates of dark biotite. Corroded crystals of calcic plagioclase and clinopyroxene with broad mantles of more sodic feldspar and amphibole, respectively, are clearly xenocrysts derived from the assimilation of gabbro. Aggregates of biotite, intergrown with pyroxene and subhedral.opaque ore similarly are interpreted as a product of reaction between the syenite magma and more mafic material, and all stages in the

Fig. 6: Total alkali versus silica diagram showing comparison between the *syenites* and *quartz syenites* of Okenyenya igneous complex.

latter's assimilation are evident within the quartz syenite. Some intrusions are thoroughly choked with extraneous material and in these cases the appearance is of a heterogeneous rock varying between a pale-coloured enclave-rich rock to a darker rock veined by pale syenite. It is evident from such intrusions that incorporation and partial assimilation of a more mafic component by the *quartz syenite* magma has taken place on a major scale.

TABLE 8: Comparison of major and trace element compositions of the *syenites* and *quartz syenites* from the Okenyenya igneous complex. Sample localities are shown in Fig. 2. nd = not detected; Fe_2O_3 calculated using $Fe_2O_3/FeO = 0.20$; L.O.I. = loss on ignition.

	Peripheral Ring Dyke SYENITE		Johannes Berg Dyke SYENITE		Johannes Berg Dyke QUARTZ SYENITE	
Sample No.	OKJ-132	OKJ-164	OKJ-124	OKJ-138	OKJ-111	OKJ-112
SiO_2	62.24	65.22	60.52	62.40	64.36	64.52
TiO_2	0.90	0.82	0.89	0.75	0.57	0.37
Al_2O_3	15.52	14.74	16.87	16.92	17.48	18.14
$Fe_2O_3$1	0.91	0.77	0.93	0.76	0.65	0.46
FeO	6.10	5.16	4.64	3.81	3.27	2.31
MnO	0.23	0.15	0.23	0.14	0.09	0.07
MgO	0.67	0.95	0.79	0.68	0.50	0.44
CaO	2.65	2.29	2.06	1.76	1.24	1.18
Na_2O	4.42	3.75	5.29	5.19	5.11	5.52
K_2O	5.26	4.96	5.89	6.07	6.43	6.79
P_2O_5	0.20	0.20	0.22	0.15	0.09	0.14
L.O.I.	0.62	0.90	1.56	1.19	0.60	0.39
TOTAL	100.70	99.73	99.88	100.00	100.44	100.40
Zr	179	347	88	127	765	550
Nb	40	39	43	56	127	91
Y	39	51	21	27	66	46
Rb	106	165	76	99	149	144
Ba	2896	1363	1135	2022	637	690
Sr	133	130	12	133	84	113
Co	nd	7	nd	nd	2	3
Cr	10	13	nd	nd	3	5
Ni	nd	3	nd	nd	nd	2
V	nd	27	nd	nd	6	7
Zn	116	93	68	84	67	43
Cu	5	8	3	6	6	8
Sc	12	12	10	5	6	4

Geochemistry

Whole-rock analyses have been undertaken on 25 acid rocks from the Okenyenya igneous complex (2 to 3 kg of 'fresh' material was collected for each sample). Analyses representative of the full range of compositions are presented in Tables I and 8. Individual analyses are available from the authors on request.

Major elements

The intrusive syenitic rocks show a range of SiO_2 content from approximately 58 - 69 wt % (Table 1; Fig. 6), there being a spread of values within each of the two rock types. The syenite occupies the lower part of the range. There is no major break in SiO_2 composition, but most samples are effectively separated at 63 wt % (Fig. 6), and significant differences between the two rock types are to be found in other components. TiO_2 is higher in the syenites (0.8 - 1.5 wt %) compared to the quartz syenites (0.3 - 0.8 wt %) mirroring the observed prevalence of ilmenite and magnetite, respectively (Ta-

ble 1). The quartz syenites have a generally lower FeO content than the syenites (4.5 - 7.5 vs 2.7 - 5.1 wt % FeO*), in spite of the fact that FeO may be increased somewhat by the presence of extraneous mafic material in the former. There are less consistent differences in the contents of other major and minor elements, although MgO, Na_2O and P_2O_5 tend to be slightly higher in the *syenites* relative to the *quartz syenites* (Table 8). Compositions of the two rock types are compared in Fig. 6.

Trace elements

Unlike the major elements which normally show close uniformity of concentration between different samples from a single intrusive sheet, trace elements may vary considerably (Table 8). A wide variability of Zr may be attributed to the uneven distribution of accessory zircon. Ba and Sr, compatible elements in feldspar (Long, 1978), show extremely erratic variations. BaO contents of 1.9 wt % have been recorded in metasomatic biotites from gabbros adjacent to syenitic intrusions at Okeny-

enya (Watkins and le Roex, unpublished data). Alteration of the syenites by the same fluids that have affected the gabbros may have locally modified the trace element concentrations whilst not significantly changing the major elements.

Despite uncertainties arising from the variability of the trace element compositions, it is evident that the high field strength elements, Zr, Nb, and Y, are significantly more concentrated in samples of *quartz syenite* than in the *syenites* (Table 8), and show good correlations with SiO_2. Sr is highly variable (5 - 310 ppm) and shows no meaningful variation between the two rock types; Ba, whilst similarly variable (~300 - 8000 ppm), generally exceeds 1000 ppm in the *syenites* but is below 1400 ppm in the *quartz syenites*. V is generally <5 ppm in the *syenites* but somewhat more enriched (maximum ~35 ppm) in the *quartz syenites*. This slight enrichment of V, together with its quite variable concentration in the *quartz syenites*, may be explained by contamination by gabbro, since V partitions strongly into magnetite (Luhr & Carmichael 1980). The effects of such contamination on the more abundant FeO and TiO_2 would not be appreciable.

Rare-earth elements

The rare-earth elements (REE) have proved especially useful in characterising the *syenites* and *quartz syenites*. Absolute concentrations of REE vary greatly, reflecting the varying degrees of differentiation within, as well as between, the two rock types. Further variability may be expected on account of the generally coarse grain size of the rocks and the irregular distribution of potentially REE-bearing apatite and zircon. REE concentrations are significantly greater in the *quartz syenites* (56 - 89 ppm La) than in the *syenites* (15 - 57 ppm

Fig. 7: Characteristic chondrite-normalised REE plots of *syenite* and *quartz syenite*. REE abundances have been normalised to chondrite values of Leedy/1.2 (Masuda *et al.*, 1972).

La), in keeping with the higher abundances of other incompatible elements. The characteristic chondrite-normalised pattern of the *quartz syenites* (Fig. 7) displays a marked negative Eu anomaly, whereas that of the *syenites* exhibits a significant positive Eu anomaly. Such distinctive profiles have been recorded, without exception, from a total of 10 *syenite* and 8 *quartz syenite* samples from different intrusions. They not only serve to underline the compositional differences between the two syenite types, but point to a significantly different petrogenesis.

Emplacement mechanisms

Ring dyke

Excluding the younger nepheline syenite intrusions of Okenyenya Berg (Fig. 2), the syenite ring dyke roughly delimits the intrusive complex at the present level of exposure. The major fracture up which the dyke was intruded forms a continuous ring comparable in scale to ring fractures at major volcanic centres on which considerable vertical displacement can be proven (MacDonald, 1972). The near-vertical, locally inward-dipping attitude of the ring dyke is typical of similar intrusions from such centres (McDonald, 1972; Taubemeck, 1967). At Okenyenya there is no direct evidence for the precise scale or direction of the vertical movement along the ring fault.

The ring fault presented a route for the rise of syenitic magma, with stoping of wall rocks possibly playing a role in widening the pathway, but injection of the magma along the fault was clearly irregular. Along much of the eastern sector it appears that only metasomatising, volatile fluids infiltrated the ring fracture. The more shallow dip of the western section of the ring fault and/or increased subsidence of this sector of the central block can account for the increased space and easier access of magma.

The plug-like body of syenite adjacent to the ring dyke at the northwestern edge of the complex is interpreted as the remains of a conduit, sited on the ring fault, up which the flow of syenite magma was concentrated.

The "ridge syenite"

There is little available field evidence to elucidate the formation of the solitary "ridge syenite". Whereas this dyke is of similar composition to that of the ring dyke and abuts the southern boundary of the igneous complex (Fig. 2), it traverses gabbros within the complex and does not occupy the main ring fracture. The intrusion could have utilised a fracture, developed as a result of flexing of a collar of sheeted tholeiitic gabbros skirting the massive core of the alkali gabbro intrusion of Martin, during subsidence of the central region of the complex.
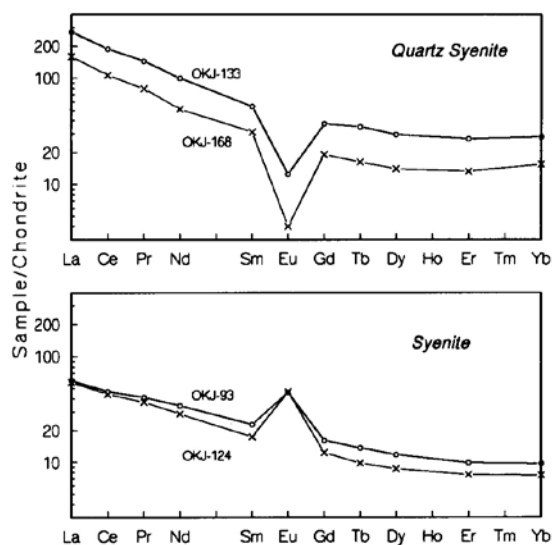
Johannes Berg syenite sheets

The arcuate dykes on Johannes Berg have a consistent outward dip of ~55° along their central segments where they parallel the neighbouring major ring dyke. The dip of the dykes steepens along their lengths and they do not extend parallel to the main ring dyke but describe a tighter arc: in the west, they extend into, or terminate against, the main ring fracture, whereas to the east they coalesce in a NNE-SSW fracture plane immediately west of Martin (Fig. 2). On the previous geological map (Simpson, 1952, 1954) a presumed fault extends along this NNE-SSW line, dividing the outcrops of the alkali gabbros of Martin and the rocks on Johannes Berg and extending across the margin of the igneous complex. We believe the NNE-SSW fracture to be continuous with the curved fractures occupied by the syenitic dykes of Johannes Berg (Fig. 2) and see no evidence for the extension of a linear fault to the SSW. Interestingly, however, Simpson (1952) suggested that the dip of layering within the gabbros shall owed on

the western side of the "fault", which is consistent with hingeing along the main arcuate fracture.

We suggest that the central core of the complex suffered non-uniform tensional stress and distortion during subsidence along the ring fault. A series of six, or more, arcuate fractures developed in response to a downward flexing of the gabbro sheets in the region of Johannes Berg (Fig. 8) and were subsequently invaded by syenitic magmas. Opening of the arcuate fractures involved vertical displacement and/or lateral slip along the NNE-SSW line, and maximum development of the dyke occurred where the fracture planes were most inclined. The shallow outward-dipping syenitic sheets on Johannes Berg appear to occupy fractures produced by sliding in the direction of extension (Fig. 8). It is possible that these low-angled slide planes in part follow boundaries between tholeiitic gabbro sheets, which prior to subsidence probably had a shallow inward dip (Simpson 1952, 1954) (Fig. 8).

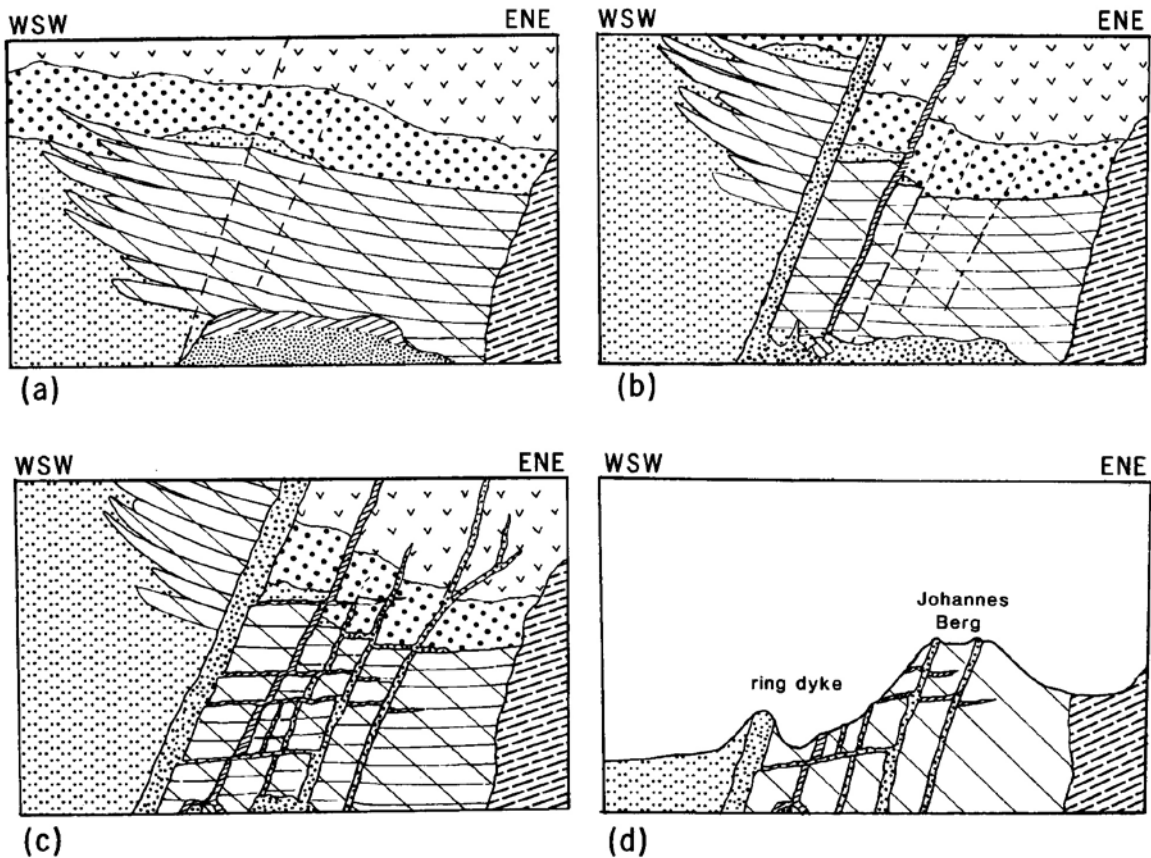The tight curvature of the dykes when compared to that of the main ring dyke reflects a different focus of

Fig. 8: Schematic cross-section through the WSW portion of Okonyenya igneous complex illustrating the proposed emplacement model for the subvolcanic syenitic intrusions of Johannes Berg. Rock types are depicted as in Fig. 2. Vertical scale is much exaggerated. The sense and extent of movement on the various faults is merely speculative, as there are no stratigraphic markers within the tholeiitic gabbro sequence on Johannes Berg. **a.** Stresses resulting from emplacement of a syenitic magma body at shallow depth beneath Okenyenya volcano produce a major concentric fracture. **b.** Evacuation of the magma chamber, possibly, but not necessarily, via the major concentric fracture, leads to a cauldron collapse. Tensional stresses resulting from vertical subsidence along the inclined ring fracture produce stress within the foundering block and sympathetic faulting. Magma is injected along faults that intersect the magma chamber. **c.** Lateral tensional stresses, together with the vertical magma injection, facilitate sliding on shallow-inclined planes, possibly coincident with the boundaries of tholeiitic gabbro sheets. **d.** Present-day erosion levels intersect the series of intrusive sheets.

concentric faulting. Tectonic focus, along with eruption site, typically migrates during the evolution of major volcanoes (McDonald, 1972). In this case, the change and localisation of the syenitic intrusions in the southwestern part of the foundered block may have been controlled by the presence of massive bodies of alkali gabbro forming Martin and Korn (Fig. 2). It is suggested that the sheeted tholeiitic gabbros underlying Johannes Berg may have more readily succumbed to tensional stresses during subsidence than the highly competent and deep-rooted alkali gabbros.

Discussion

The Okenyenya igneous complex pierces subhorizontal sedimentary strata of Karoo age. The sedimentary rocks have been recrystallised and locally melted adjacent to the gabbro intrusions and several metamorphosed rafts of conglomerate are presently exposed inside the complex (Fig. 2). The Karoo rocks are some 200 m thick on the Otjukundu Plateau, south of the complex, where they have been protected from erosion by sills of resistant granophyre which cap the plateau. It is presumed that removal of a considerable thickness of Karoo sediments, and probably also Etendeka volcanics (Milner & Ewart, 1989; Milner *et al.*, *in press*), has taken place in the vicinity of the Okenyenya complex, erosion having been particularly swift during the period of coastal uplift following continental break-up (Brown *et al.*, 1990). Nevertheless, it is uncertain whether the thickness of Karoo rocks present at the time of intrusion of the complex could have greatly exceeded the maximum of 600 m presently preserved in the region (Gevers, 1936).

The hills of Korn and Martin (Fig. 2) form the remains of significant magma chambers which solidified slowly at depth to produce coarse-grained, partially layered, gabbros. Today these peaks lie a mere 100m and 150 m, respectively, beneath the most elevated Karoo rocks (1430 m) on the southern rim of the complex (Fig. 2). (The younger nepheline syenite intrusions of Okenyenya Berg, equally clearly plutonic in origin, presently project 500 m above the surrounding Karoo strata). There being evidence neither for major thicknesses of superimposed strata in the late-Mesozoic nor for large-scale resurgence of the complex (Smith & Bailey, 1968; Hon & Fridrich, 1989), the presence of plutonic intrusions close to the surface is best explained by their intrusion into the base of a major volcano. The magma chambers could have been formed in, or partially within, a volcanic pile which may have been a few thousand metres high and laterally extensive.

The outward dip of the syenitic sheets in the WSW part of the complex and the clear tensional nature of the faulting that allowed magma intrusion indicate that subsidence has occurred, at least in this part of the complex. The presence of the major ring fracture at depth in the igneous complex is correlated to cauldron formation in the overlying volcano. Cauldron collapse is characteristically associated with major eruptions of magmas that are frequently syenitic (trachytic) in character. The apparent structural relations between the numerous syenitic intrusions discussed in this study indicate that their emplacement may result from a major cauldron subsidence of a former Okenyenya volcano, and they may, consequently, be essentially coeval.

A tentative model for the emplacement of the intermediate and acid rocks of Okenyenya is summarised as follows (see Fig. 8):

- a major body of syenite magma was introduced at shallow depth beneath a large basaltic Okenyenya volcano;
- magmatic pressure produced tumescence and the formation of a major circular fracture along which cauldron collapse of a central region of the volcano subsequently took place, after expulsion of syenitic magmas;
- an outward dip of the western segment of the ring fault plane and a downward flexing of the roof of the magma chamber in the western half of the complex gave rise to maximum tension in this part of the foundering block;
- syenite magma rose most readily up the western segment of the ring fracture and invaded a complex series of tensional fractures developed in the brittle roof zone to produce the sheet intrusions of Johannes Berg;
- movement of syenite magma became focused at a point on the northwestern side of the ring fracture with development of a steep-walled conduit;
- failure within the sheeted tholeiitic gabbros around the southern margin of the massive intrusion of Martin caused the opening of a single fracture that was invaded by magma to form the "ridge syenite";
- magma was injected at localised sites around the eastern part of the ring fracture, but much of the fracture in this region saw the passage only of fluids, resulting in metasomatism of the gabbro rocks immediately adjacent to the fracture.

The model for emplacement, outlined above, is consistent with present field evidence and provides a unifying mechanism for the formation of the very numerous syenitic intrusions in the Okenyenya igneous complex. A full discussion on the genesis of the *syenite* and *quartz syenite* magmas and their relationships to other magmas of the complex is beyond the scope of this paper. Nevertheless, in order for the emplacement model to be tenable, it must allow for the injection, at closely related times, of syenitic magmas of two differing compositions. Furthermore, the model must account for the heterogeneous nature of the *quartz syenite* with its abundant mafic inclusions. For these reasons, there follows a brief discussion on aspects of the syenite petrogenesis.

It cannot be discounted that two bodies of syenitic magma of separate origin existed beneath Okenyenya

around the time of cauldron collapse, and were tapped by faulting resulting from the subsidence of the central part of the complex. Recurrent subsidence or merely stress induced by the initial collapse could have produced fracturing, facilitating the intrusion of a second magma later than the first, so producing the close spacial association of the two syenite types. Alternatively, the presence of two magmatic compositions within the very closely spaced and localised dykes and sills of Johannes Berg might be explained by their coexistence within a single differentiated magma chamber. A degree of compositional variation within a syenite magma chamber is suggested by differences in the chemical composition of *syenite* from relatively closely spaced localities on the ring dyke (Table 8).

The contrasting rare-earth element signatures of the syenite and *quartz syenite* point to profound differences in their evolutionary history. The negative Eu anomaly exhibited by the *quartz syenites* is typical of that widely recorded in syenitic rocks and presumed to originate through feldspar fractionation during evolution from basaltic parent magmas. The positive Eu anomalies recorded in all analysed samples of *syenite* from the complex is evidence that generation of this magma involved significant feldspar accumulation. The relatively small amount of plagioclase feldspar present in the rock and the small normative anorthite component implies that alkali feldspar accumulation was the major mechanism of Eu enrichment (Schnetzler & Philpotts, 1970; Nagasawa, 1973). It is highly improbable that large degrees of feldspar fractionation could have taken place within the relatively small sheet intrusions and there is no evidence of cumulate textures within the *syenite* dykes and sills. At the time of intrusion, the *syenite* magma presumably contained a high proportion of feldspar crystals. The aphyric nature of narrow offshoots from the *syenite* sheets (Fig. 3) may be explained by mechanisms such as filter pressing and possibly flow differentiation.

Removal of alkali feldspar from a syenitic magma would enhance any negative Eu anomaly in the liquid, placing constraints on the possible generation of the *syenite* and *quartz syenite* as complementary portions of a formerly homogeneous body of syenite magma. *Syenite* is considerably the more voluminous of the two syenitic rocks in the complex and preserved volumes of *quartz syenite* might appear too small to equate with the relative sizes of Eu anomalies if produced through feldspar loss to the *syenite*. However, it is certain that very large volumes of magma were released at the time of cauldron formation and it is unlikely that the true volume relations of the two magmas have been preserved.

Geochemically, the *quartz syenite* represents a more evolved magma enriched in incompatible elements and volatile components. However, the lower content of highly charged "incompatible" trace elements Zr, Nb, Y and REE, and reduced MgO in the *syenite* may simply reflect the dilution of the magma by large amounts of cumulate feldspar. Presence of amphibole and biotite, rather than clinopyroxene and fayalite, in the *quartz syenite* is consistent with somewhat increased volatile content of this magma. The significantly greater degree of sericitic breakdown of the alkali feldspars and the prevalence of this alteration at the margins of the crystals further indicates the influence of volatiles. It is possible that a volatile- and incompatible element-enriched *quartz syenite* liquid developed in the upper portions of a syenitic magma chamber undergoing major feldspar fractionation.

The abundant wall-rock fragments in the marginal zones of all the major syenitic intrusions (Fig. 4d) originate from brecciation along the fault planes preceding their invasion by magma. Whereas chemical stoping may have been important in widening the fractures and facilitating further intrusion, it cannot account for the ubiquitous clots of mafic material in the *quartz syenite* intrusions, and local dense concentrations of extraneous rock fragments. The thermal budget of the thin intrusive sheets would have been insufficient to promote significant melting and assimilation of gabbroic wall rocks and, accordingly, wall-rock xenoliths remain largely angular with limited reaction coronas. Despite this fact, the abundant aggregates of biotite and xenocrysts of augite and labradorite are clearly a residue from a more comprehensive reaction between gabbro and the *quartz syenite* magma. Well-rounded enclaves of biotite-rich rock that occur in profusion in the *quartz syenite* intrusions point to a significant degree of assimilation and recrystallisation of a mafic rock that must have taken place within a magma chamber of significant size. The large-scale reaction may have involved the injection of a gabbroic magma into a chamber of syenite magma, as has been invoked elsewhere as a triggering mechanism for major volcanic eruptions and cauldron formation. Alternatively, major assimilation of gabbroic rocks might have been possible by a *quartz syenite* liquid accumulated at the roof of a large syenite magma chamber and continuously recharged by the upward migration of heat and volatiles.

Summary

Although dwarfed in volume by gabbroic rocks, the intermediate to acid rocks constitute a significant component of the Okenyenya igneous complex. Detailed geological mapping of the complex has invalidated the former suggestion (Simpson, 1954) that these rocks were emplaced as a single shell around older gabbroic intrusions. Instead they form numerous discrete intrusive sheets, both at the margin and also within the gabbroic core of the complex. They essentially comprise two compositions, *syenite* and *quartz syenite* (Le Maitre, 1989), with more quartz-rich micro granites restricted to relatively minor dykes. Whilst there is broad continuity of composition between the two rock types, the trace element composition, especially the REE, and

the contrasting presence or absence of mafic enclaves point to significant differences in the formation of the two magma types.

Despite this conclusion, it is possible to model the structure of the very numerous *syenite* and *quartz syenite* intrusions as a response to cauldron subsidence within the complex, arguing for the broadly coeval nature of the intrusions. A possible model for emplacement of the syenitic rocks involves the tapping of a magma chamber in which a *quartz syenite* liquid had accumulated through significant fractionation of alkali feldspar and volatile migration. Such a magma appears to have been capable of actively stoping gabbros, so producing the exceptional abundance of mafic debris in the *quartz syenite*, and/or to have itself been intruded by a more mafic liquid, possibly triggering major syenitic volcanism and associated cauldron collapse. Detailed geochemical studies of the two syenite rock types and of associated gabbros are presently underway to assess the validity of such a model and to elucidate further the role of the syenites in the overall evolution of the complex.

Acknowledgements

References

Albee, A.L. and Ray, L. 1970. Correction factors for electron probe microanalysis of silicates, oxides, carbonates, phosphates, and sulfates. *Analyt. Chem.*, **42**, 1408-1414.

Bence, A.E. and Albee, A.L. 1968. Empirical correction factors for the electron microanalysis of silicates and oxides. *J. Geol.*, **76**, 382-403.

Brown, W.R., Rust, D.J., Summerfield, M.A., Gleadow, AJ.W. and De Wit, M.C.J. 1990. An early Cretaceous phase of accelerated erosion on the south-western margin of Africa: evidence from apatite fission track analysis and the offshore sedimentary record. *Nucl. Tracks Radiat. Meas.*, **17**, 339-350.

Duncan, A.R., Erlank, A.J. and Betton, P.J. 1984. Appendix I Analytical techniques and database descriptions. *Spec. Publn geol. Soc. S. Afr.*, **13**, 389-395.

Gevers, T.W. 1936. The Etjo beds of northern Hereroland. *Trans. geol. Soc. S. Afr.*, **39**, 317-329.

Hon, K. and Fridrich, C. 1989. How calderas res urge. *In*: *Continental Magmatism*. Abstr. Bull. New Mexico Bur. Mines & Min. Resour., **131**, 135.

Korn, H. and Martin, H. 1939. Junge vulkano-plutone

in Südwestafrika. *Geol. Rdsch.*, **30**, 631-636.

Le Maitre, R.W. 1989. *A classification of igneous rocks and glossary of terms*. Blackwell, Oxford, 193 pp.

Le Roex, A.P. and Watkins, R.T. 1990. Analysis of rare-earth elements in geological samples by gradient ion chromatography: An alternative to ICP and INAA *Chem. Geol.*, **88**, 151-162.

Leake, B.E. 1978. Nomenclature of amphiboles. *Am. Miner.*, **63**, 1023-1052.

Long, P.E. (1978) Experimental determination of partition coefficients for Rb, Sr, and Ba between alkali feldspar and silicate liquid. *Geochim. cosmochim. Acta*, **42**, 833-846.

Luhr, J.F. and Carmichael, I.S.E. 1980. The Colima Volcanic Complex, Mexico. L Post-caldera andesites from Volcan Colima. *Contr. Miner. Petrol.*, **71**, 343-372.

MacDonald, G.A. 1972. *Volcanoes*. Prentice-Hall, New Jersey, 510 pp.

Masuda, A., Nakamura, N. and Tanaka, T. 1973. Fine structures of mutually normalised rare-earth patterns of chondrites. *Geochim. cosmochim. Acta*, **42**, 833-846.

Milner, S.C. and Ewart, A. 1989. The geology of the Goboboseb Mountain volcanics and their relation to the Messum Complex, Namibia. *Communs geol. Surv. Namibia*, **5**, 31-40.

Milner, S.C., Duncan, A.R. and Ewart, A. (*in press*) Quartz latite rheoignimbrite flows of the Etendeka Formation, north-western Namibia. *J. Volcanol. geotherm. Res.*

Morimoto, N., Fabries, J., Ferguson, A.K., Ginzburg, L.V., Ross, M., Seifert, F.A., Zussman, J., Aoki, K. and Gottardi, G. 1988. Nomenclature of pyroxenes. *Am. Miner.*, **73**, 1123-1133.

Nagasawa, N. 1973. Rare-earth distribution in alkali rocks from Oki-Dogo Island, Japan. *Contr. Miner. Petrol.*, **39**, 301-305.

Norrish, K. and Hutton, J.T. 1969. An accurate X-ray spectrographic method for the analysis of a wide range of geological samples. *Geochim. cosmochim. Acta*, **33**, 431-453.

Schnetzler, C.C. and Philpotts, J.A. 1970. Partition coefficients of rare-earth elements between igneous matrix material and rock-forming mineral phenocrysts - II. *Geochim. cosmochim. Acta*, **34**, 331-340.

Simpson, E.S.W. 1950. Preliminary notes on the Okonjeje igneous complex, South West Africa. *Geol. Rdsch.*, **38**, 15-18.

Simpson, E.S.W. 1952. *The Okonjeje Igneous Complex, South West Africa*. Ph.D. thesis (unpubl.), University of Cambridge, 132 pp.

Simpson, E.S.W. 1954. The Okonjeje igneous complex, South West Africa. *Trans. geol. Soc. S. Afr.*, **57**, 125-172.

Smith, R.L. and Bailey, R.A. 1968. Resurgent cauldrons. *Mem. geol. Soc. Am.*, **116**, 13-62.

Streckeisen, A. 1973. Plutonic Rocks. Classification

and nomenclature recommended by the IUGS sub-commission on the systematics of igneous rocks. *Geotimes*, **18**, 26-30.

Tauberneck, W.H. 1967. Notes on the Glen Coe cauldron subsidence, Argyllshire, Scotland. *Bull. geol. Soc. Am.*, **78**, 1295-1316.